

Electronic supplementary information

Fe-N-functionalized carbon electrocatalyst derived from zeolitic imidazolate framework for oxygen reduction: Fe and NH₃ treatment effects

Thanh-Nhan Tran, Cheol-Hwan Shin, Byong-June Lee, Jitendra Samdani, Jong-Doek Park, Tong-Hyun Kang and Jong-Sung Yu*

Department of Energy Science and Engineering, Daegu Gyeongbuk Institute of Science and Technology (DGIST), Daegu, 42988, Republic of Korea

Email: jsyu@dgist.ac.kr

Reagent and chemicals

Zinc (II) nitrate hexahydrate ($\text{Zn}(\text{NO}_3)_2 \cdot 6\text{H}_2\text{O}$, > 98.0%), 2-methylimidazole ($\text{C}_4\text{H}_6\text{N}_2$, 99%) and iron (III) acetylacetone ($\text{Fe}(\text{acac})_3$, 97%) were purchased from Sigma-aldrich (U.S.A.). Methanol (CH_3OH , 99.5%) and ethanol ($\text{CH}_3\text{CH}_2\text{OH}$, 99%) were purchased from Samchun Pure Chemical Co., Ltd. (Korea). Ultrapure water (resistance > 18 $\text{M}\Omega\text{cm}^{-1}$) was used in all experiments.



Fig. S1 Photographic images of $\text{Fe}_x\text{-N/C}$ ($x = 0.02, 0.04, 0.06$, and 0.08) precursors, which correspond to the different mixtures of $\text{Fe}(\text{acac})_3$ and ZIF-8.

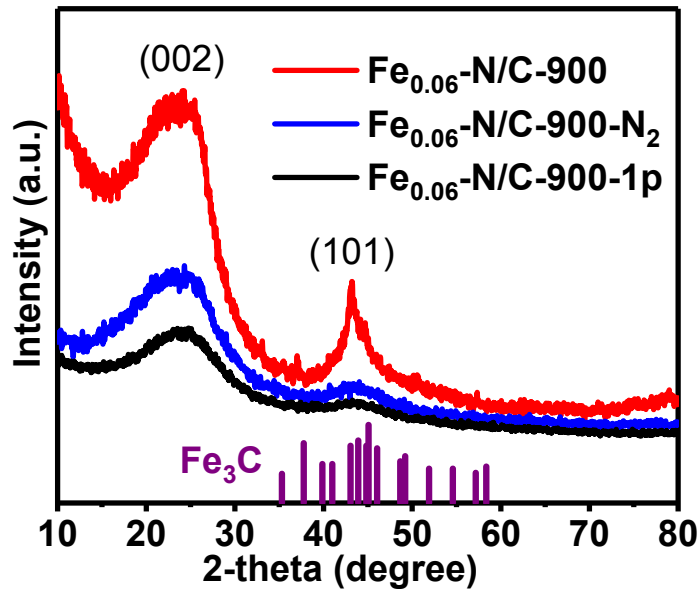


Fig. S2 XRD spectra of $\text{Fe}_{0.06}\text{-N/C-900-1p}$, $\text{Fe}_{0.06}\text{-N/C-900-N}_2$, and $\text{Fe}_{0.06}\text{-N/C-900}$.

Table S1 Physicochemical properties of all the as-prepared samples.

Samples	$S_{\text{BET}}(\text{m}^2/\text{g})$	$S_{\text{micro}}(\text{m}^2/\text{g})$	$S_{\text{micro}}/S_{\text{BET}}$	$V(\text{cm}^3/\text{g})$	I_D/I_G	I_{AM}/I_G
$\text{Fe}_{0.06}\text{-N/C-900-N}_2$	1094.0	960.6	87.8%	0.57	0.97	0.71
$\text{Fe}_{0.02}\text{-N/C-900}$	2313.4	1426.2	61.6%	1.40	0.90	0.37
$\text{Fe}_{0.04}\text{-N/C-900}$	1498.5	831.6	55.5%	1.23	0.98	0.41
$\text{Fe}_{0.06}\text{-N/C-900}$	1288.7	826.2	64.1%	0.98	1.02	0.58
$\text{Fe}_{0.08}\text{-N/C-900}$	1186.4	891.1	75.1%	0.87	0.91	0.52

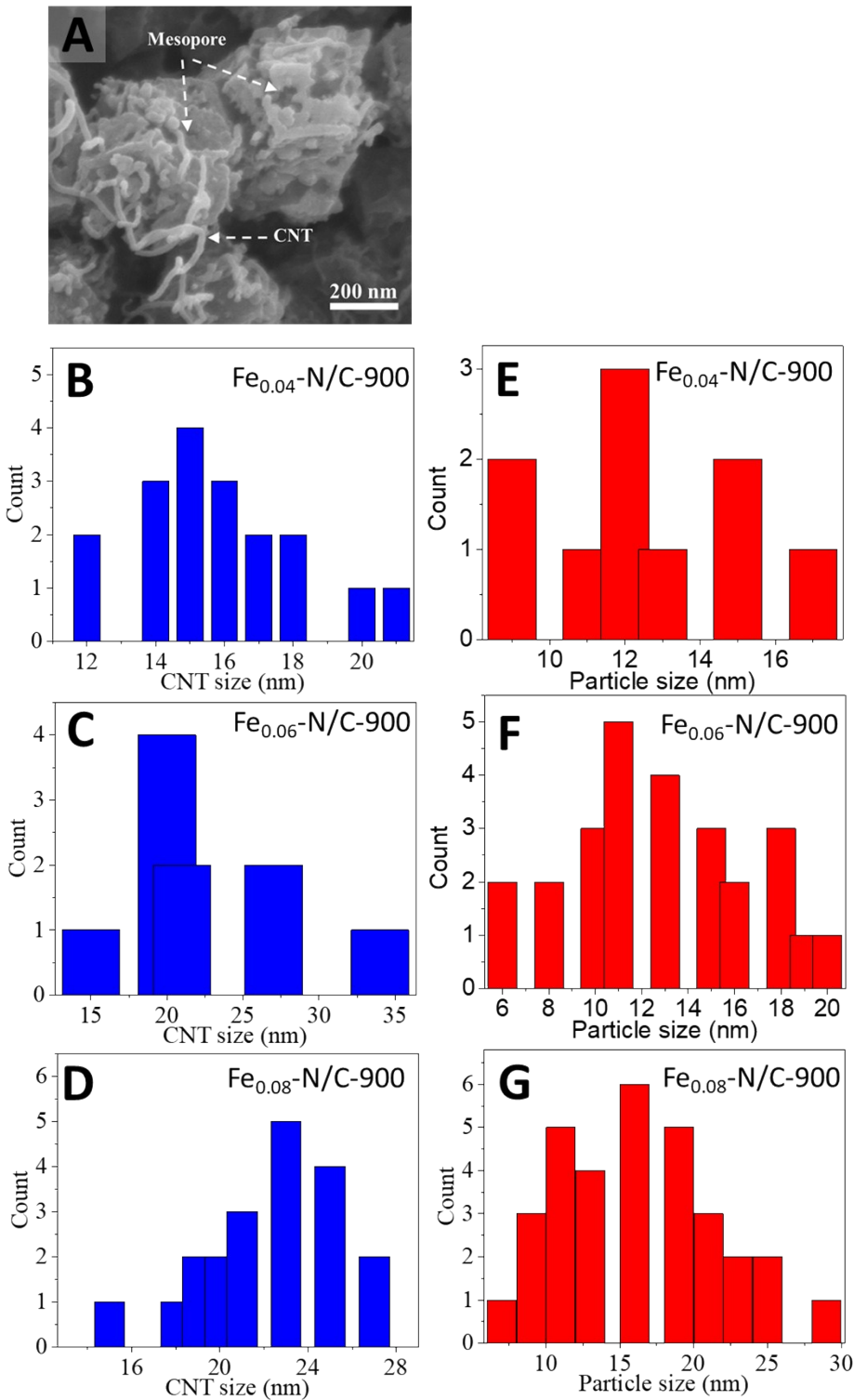


Fig. S3 A) SEM image of $\text{Fe}_{0.06}\text{-N/C-900}$ showing the development of pores and N-doped CNTs. B-D) size distribution histograms of CNTs from SEM images in Fig. 3B-D and E-G) particle size distribution from TEM images in Fig. 3F-H for $\text{Fe}_{0.04}\text{-N/C-900}$, $\text{Fe}_{0.06}\text{-N/C-900}$, and $\text{Fe}_{0.08}\text{-N/C-900}$, respectively.

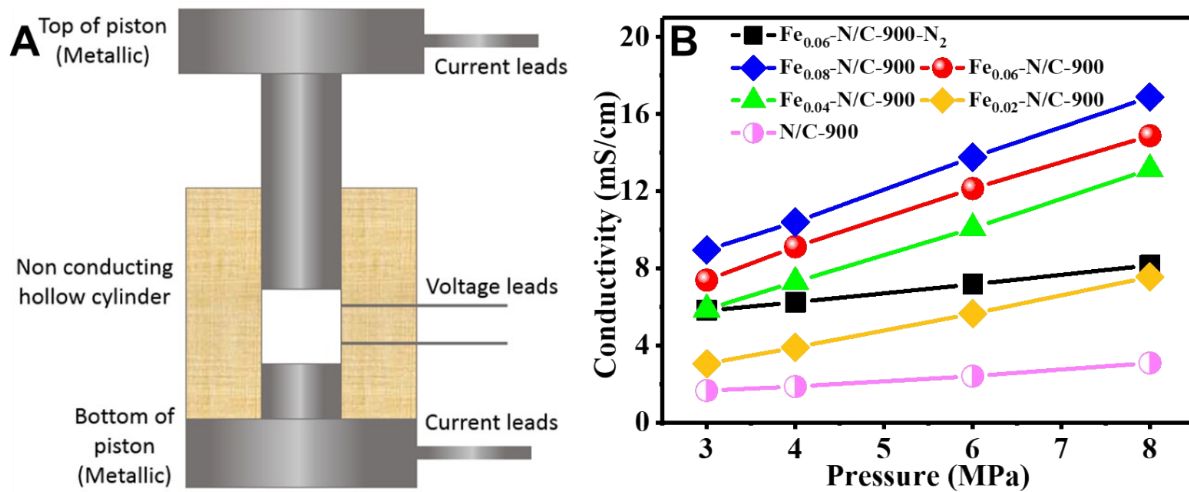


Fig. S4 A) Electrical conductivity cell with four-probe configuration, and B) electrical conductivity vs pressure profiles of $\text{Fe}_x\text{-N/C-900}$ and $\text{Fe}_{0.06}\text{-N/C-900-N}_2$.

Table S2 Atomic composition obtained from XPS spectra for the as-prepared samples.

Samples	C 1s (at. %)	Fe 2p (at. %)	N 1s (at. %)	O 1s (at. %)
$\text{Fe}_{0.06}\text{-N/C-900-N}_2$	84.13	0.18	3.93	11.76
N/C-900	88.89	N/A	3.62	7.49
$\text{Fe}_{0.02}\text{-N/C-900}$	88.68	0.23	4.36	6.73
$\text{Fe}_{0.04}\text{-N/C-900}$	88.06	0.27	5.10	6.57
$\text{Fe}_{0.06}\text{-N/C-900}$	87.27	0.37	7.12	5.24
$\text{Fe}_{0.08}\text{-N/C-900}$	87.87	0.30	5.94	5.89

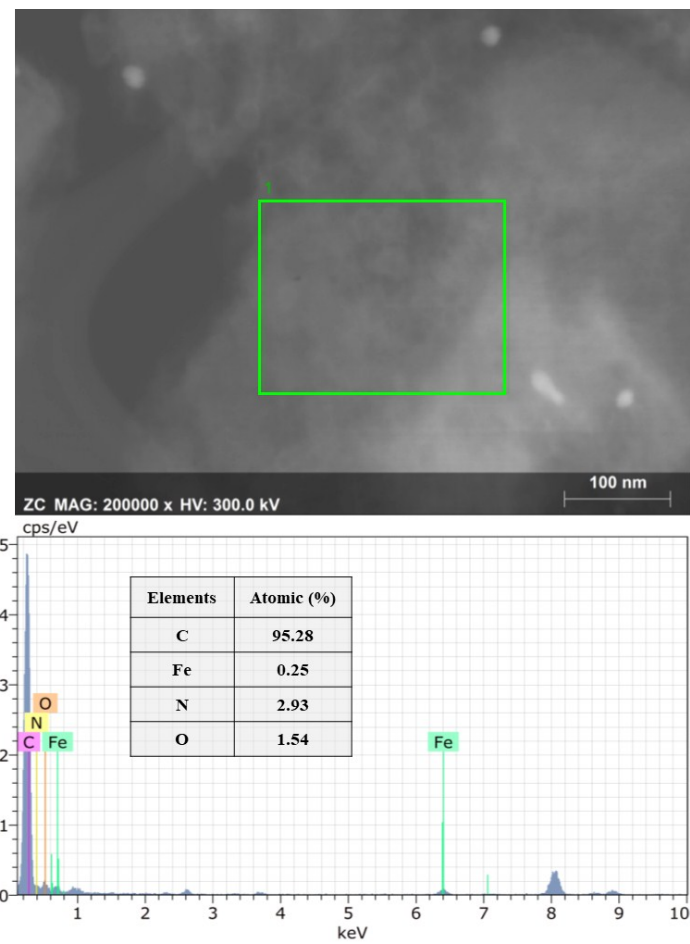


Fig. S5 STEM image and EDS spectrum of a selected area along with a table of elemental atomic percentage (inset) of $\text{Fe}_{0.06}\text{-N/C-900}$ catalyst.

Table S3 Summary of ORR activities of $\text{Fe}_{0.06}\text{-N/C-900}$ and recently reported non-precious Fe-N-C catalysts in acidic medium (electrode rotating speed 1600 rpm).

Materials	Electrolyte	$E_{\text{onset}} \text{ relative to Pt/C}$	$E_{1/2} \text{ relative to Pt/C}$	Current density at 0.15 V (vs. RHE) (mA/cm ²)	Ref.
FeNC-20-1000	0.1 M HClO_4	Negative shift ~ 70 mV	Negative shift ~ 57 mV	6.20	¹
C-Fe-Z8-Ar	0.1 M HClO_4	Negative shift ~ 70 mV	Negative shift ~ 40 mV	7.40	²
C-2PANI/PBA	0.5 M H_2SO_4	Negative shift ~ 150 mV	Negative shift ~ 100 mV	6.00	³
C-Z8Nc/FePc-900	0.1 M HClO_4	Negative shift ~ 50 mV	Negative shift ~ 50 mV	5.60	⁴
C-FeZIF-900-0.84	0.1 M HClO_4	Negative shift ~ 100 mV	Negative shift ~ 80 mV	5.70	⁵
5% Fe-N/C	0.5 M H_2SO_4	Negative shift ~ 157 mV	Negative shift ~ 39 mV	5.12	⁶
$\text{NH}_3\text{-Fe}_{0.25}\text{-N-C-900}$	0.1 M HClO_4	Negative shift ~ 110 mV	Negative shift ~ 100 mV	5.98	⁷
C-AFC© ZIF-8	0.1 M HClO_4	Negative shift ~ 80 mV	Negative shift ~ 36 mV	5.95	⁸
$\text{Fe}_{0.06}\text{-N/C-900}$	0.1 M HClO_4	Negative shift ~ 39 mV	Negative shift ~ 33 mV	6.66	This Work

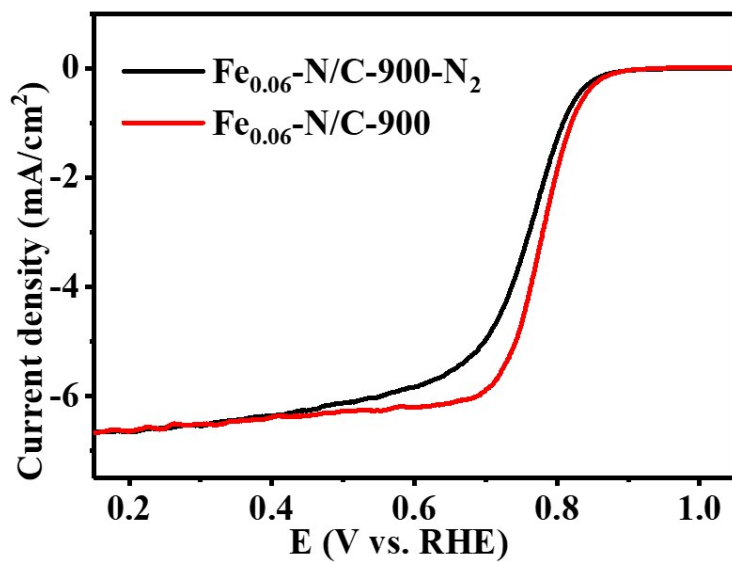


Fig. S6 LSV curves of $\text{Fe}_{0.06}\text{-N/C-900}$ and $\text{Fe}_{0.06}\text{-N/C-900-N}_2$ with rotation speed 1600 rpm at scan rate of 10 mV/s in O_2 -saturated 0.1 M HClO_4 .

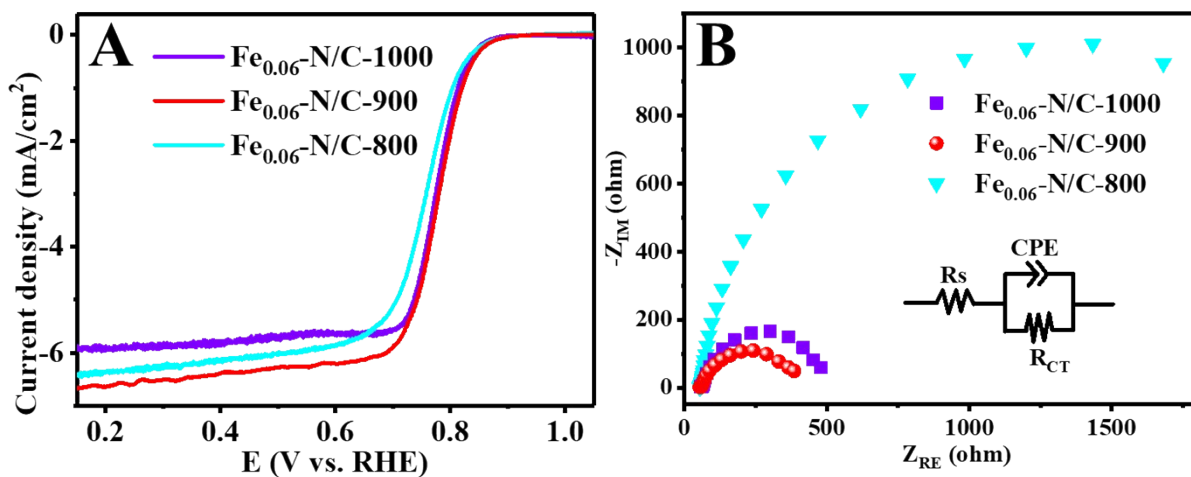


Fig. S7 A) LSV curves, and B) Nyquist plots (inset: equivalent circuits) of the $\text{Fe}_{0.06}\text{-N/C-800}$, $\text{Fe}_{0.06}\text{-N/C-900}$, and $\text{Fe}_{0.06}\text{-N/C-1000}$ prepared at different pyrolysis temperatures in O_2 -saturated 0.1 M HClO_4 .

Table S4 EIS parameters of $\text{Fe}_{0.06}\text{-N/C-T}$ obtained from analysis of Nyquist plot.

Samples	R_s (Ω)	R_{CT} (Ω)	CPE ($\text{mFs}^{1/\alpha}$)
$\text{Fe}_{0.06}\text{-N/C-1000}$	55.6	445.8	3.53
$\text{Fe}_{0.06}\text{-N/C-900}$	57.4	345.3	4.31
$\text{Fe}_{0.06}\text{-N/C-800}$	56.5	2238.0	1.62

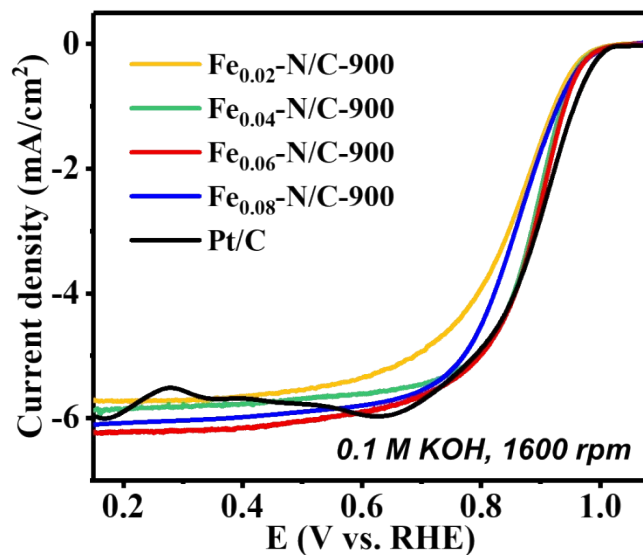


Fig. S8 LSV curves of as-prepared catalysts $\text{Fe}_x\text{-N/C-900}$ and Pt/C-TKK in O_2 -saturated 0.1 M KOH.

Table S5 Single cell performances in H₂/O₂ PEMFC of Fe_{0.06}-N/C-900 and recently reported non-precious Fe-N-C catalysts.

Materials	Precursors	Operation conditions: temperature, backpressure, cathode catalyst loading.	P _{max} (mW/cm ²)	I at 0.6 V (mA/cm ²)	Ref.
py-Fe-FA/C	FeCl ₃ , vitamin B19, carbon Vulcan.	80 °C, 1 bar, 6 mg/cm ²	330	140	⁹
Fe-N-C	Iron (II) phthalocyanine with silica template.	60 °C, 3 bar , 2.5 mg/cm ²	105	70	¹⁰
Fe-N/CNN3	Fe(ac) ₂ , 2,4,6-Tris(2-pyridyl)-s-triazine.	60 °C, 2 bar, 2.6 mg/cm ²	121	40	¹¹
Fe-NCB	Fe(NO ₃) ₃ , nicarbazin, silica template.	80 °C, 1.5 bar, 4 mg/cm ²	500	520	¹²
FeCoTETA/C	CoCl ₂ , FeCl ₂ triethylenetetramine, carbon black.	50 °C, 2 bar, 2 mg/cm ²	256	200	¹³
(CM+PANI)- Fe-C	FeCl ₃ , Cyanamide, Aniline	80 °C, 2 bar, 4 mg/cm ²	940	1100	¹⁴
Fe_{0.06}-N/C- 900	ZIF-8, Fe(acac)₃	80 °C, 2 bar, 3.5 mg/cm²	503	564	This work

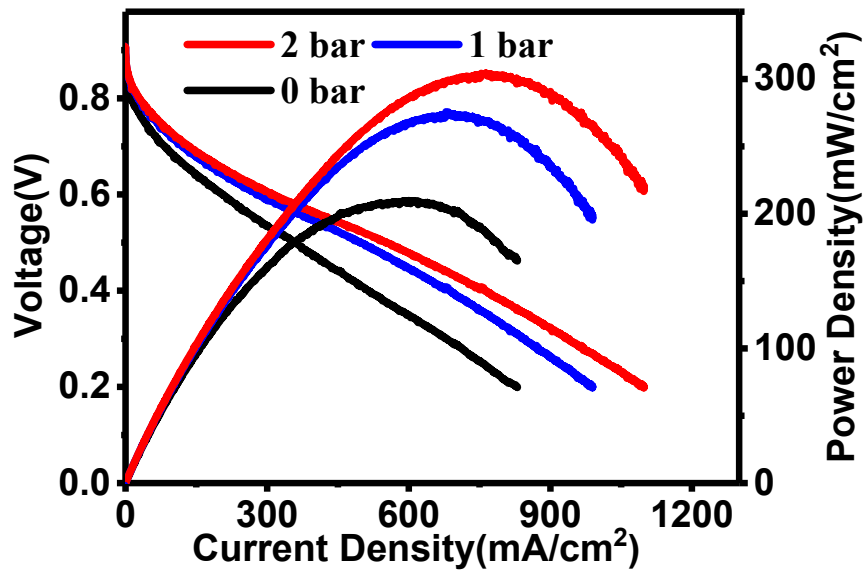


Fig. S9 H₂/air fuel cell polarization curves and corresponding power density at 80 °C with various backpressure from 0 to 2 bar (the cathode catalyst loading is 3.5 mg/cm², and membrane of MEA is nafion 212) of Fe_{0.06}-N/C-900.

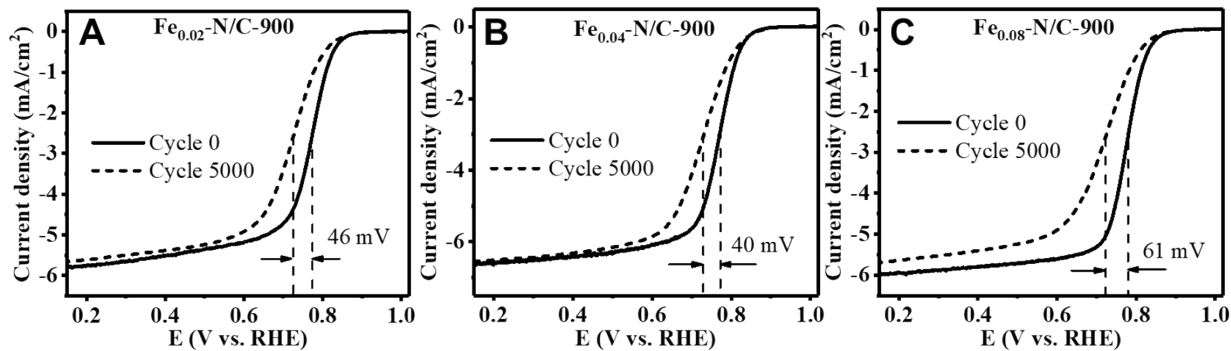


Fig. S10 LSV curves at before (cycles 0) and after 5000 potential cycles (Cycle 5000) in O₂-saturated HClO₄ of Fe_{0.02}-N/C-900, Fe_{0.04}-N/C-900 and Fe_{0.08}-N/C-900.

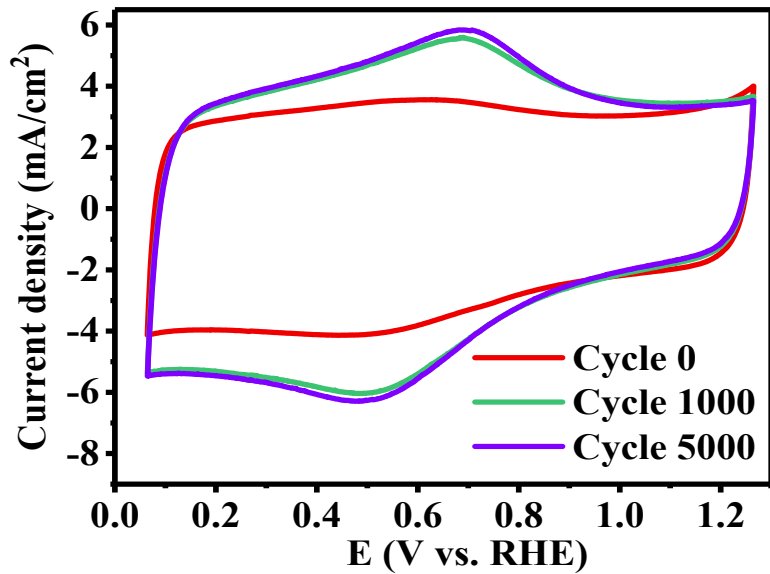


Fig. S11 Cyclic voltammograms of $\text{Fe}_{0.06}\text{-N/C-900}$ electrode in N_2 -saturated 0.1 M HClO_4 solution at different potential cycles of $N = 0, 1000, 5000$.

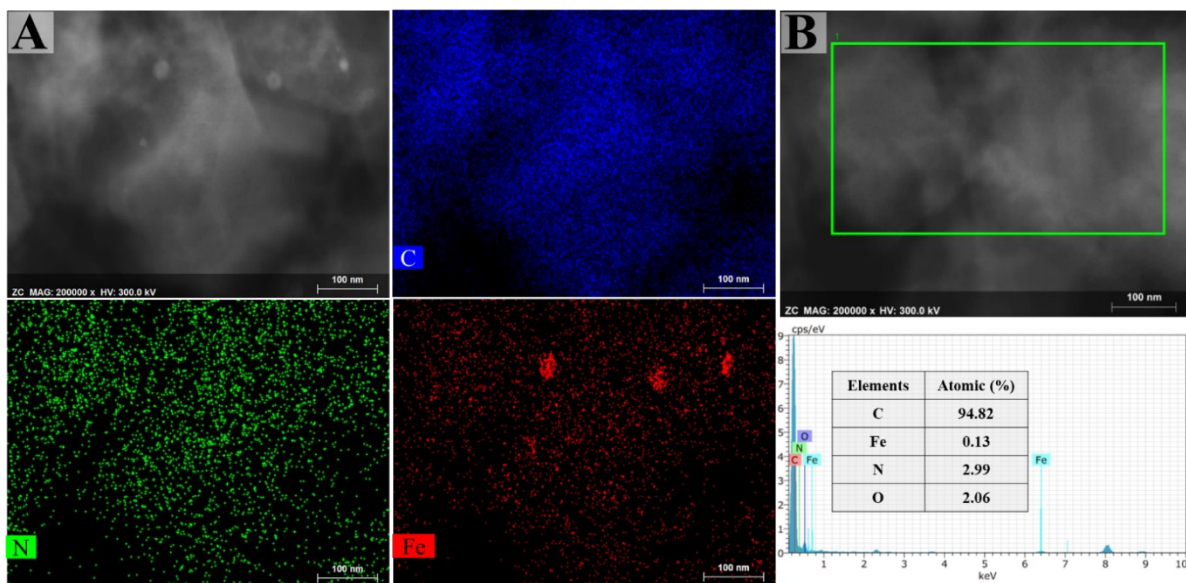


Fig. S12 A) STEM images with elemental mapping for C, N, and Fe, and B) a selected area EDS spectrum with a table of elemental atomic percentages (inset) of $\text{Fe}_{0.06}\text{-N/C-900}$ sample after 5000 potential cycles.

References

- 1 T. Liu, P. Zhao, X. Hua, W. Luo, S. Chen and G. Cheng, *J. Mater. Chem. A*, 2016, **4**, 11357–11364.
- 2 X. Wang, H. Zhang, H. Lin, S. Gupta, C. Wang, Z. Tao, H. Fu, T. Wang, J. Zheng, G. Wu and X. Li, *Nano Energy*, 2016, **25**, 110–119.
- 3 X. Wang, L. Zou, H. Fu, Y. Xiong, Z. Tao, J. Zheng and X. Li, *ACS Appl. Mater. Interfaces*, 2016, **8**, 8436–8444.
- 4 R. Zheng, S. Liao, S. Hou, X. Qiao, G. Wang, L. Liu, T. Shu and L. Du, *J. Mater. Chem. A*, 2016, **4**, 7859–7868.
- 5 Y. Deng, Y. Dong, G. Wang, K. Sun, X. Shi, L. Zheng, X. Li and S. Liao, *ACS Appl. Mater. Interfaces*, 2017, **9**, 9699–9709.
- 6 Q. Lai, L. Zheng, Y. Liang, J. He, J. Zhao and J. Chen, *ACS Catal.*, 2017, **7**, 1655–1663.
- 7 H. Tan, Y. Li, X. Jiang, J. Tang, Z. Wang, H. Qian, P. Mei, V. Malgras, Y. Bando and Y. Yamauchi, *Nano Energy*, 2017, **36**, 286–294.
- 8 Y. Ye, F. Cai, H. Li, H. Wu, G. Wang, Y. Li, S. Miao, S. Xie, R. Si, J. Wang and X. Bao, *Nano Energy*, 2017, **38**, 281–289.
- 9 H.-C. Huang, S.-T. Chang, H.-C. Hsu, H.-Y. Du, C.-H. Wang, L.-C. Chen and K.-H. Chen, *ACS Sustain. Chem. Eng.*, 2017, **5**, 2897–2905.
- 10 L. Osmieri, R. Escudero-Cid, A. H. A. Monteverde Videla, P. Ocón and S. Specchia, *Appl. Catal. B Environ.*, 2017, **201**, 253–265.
- 11 E. Negro, A. H. A. M. Videla, V. Baglio, A. S. Aricò, S. Specchia and G. J. M. Koper, *Appl. Catal. B Environ.*, 2015, **166–167**, 75–83.
- 12 A. Serov, K. Artyushkova, E. Niangar, C. Wang, N. Dale, F. Jaouen, M. T. Sougrati, Q. Jia, S. Mukerjee and P. Atanassov, *Nano Energy*, 2015, **16**, 293–300.
- 13 H. J. Zhang, X. Yuan, L. Sun, J. Yang, Z. F. Ma and Z. Shao, *Electrochim. Acta*, 2012, **77**, 324–329.
- 14 H. T. Chung, D. A. Cullen, D. Higgins, B. T. Snead, E. F. Holby, K. L. More and P. Zelenay, *Science (80-.).*, 2017, **357**, 479–484.